

# A gas and dust rich giant elliptical galaxy in the ISOPHOT Serendipity Survey<sup>★</sup>

O. Krause<sup>1</sup>, U. Lisenfeld<sup>2</sup>, D. Lemke<sup>1</sup>, M. Haas<sup>1</sup>, U. Klaas<sup>1</sup>, and M. Stickel<sup>1</sup>

<sup>1</sup> Max-Planck-Institut für Astronomie, Königstuhl 17, 69117 Heidelberg, Germany

<sup>2</sup> Instituto de Astrofísica de Andalucía, Camino Bajo de Huetor 24, 18080 Granada, Spain

Received 12 February 2003 / Accepted 9 March 2003

**Abstract.** We present a multi-wavelength study of the unusual galaxy ISOSS J 15079+7247. With a bolometric luminosity of  $L_{\text{FIR}} \sim 2 \times 10^{12} L_{\odot}$  this object is one of the most luminous galaxies detected by the 170  $\mu\text{m}$  ISOPHOT Serendipity Survey (ISOSS). We have obtained 1.2 mm continuum and CO (1–0) line observations, optical spectra and deep  $R$ -band images of the system. The CO emission originates from a giant elliptical galaxy at redshift  $z = 0.2136$ , yielding a molecular gas mass of  $2.9 \times 10^{10} M_{\odot}$ . The high gas mass favors the picture that the dust emission is associated with the elliptical galaxy. The nature of the ultraluminous IR emission can be explained by an opaque, hidden starburst in the center of the elliptical. The huge dust mass of  $5 \times 10^8 M_{\odot}$  corresponds to a visual extinction of  $A_V \sim 1000$  mag. This is consistent with the non-detection of any optical signatures of a strong starburst in ISOSS J 15079+7247 and the strength of non-thermal radio continuum emission.

**Key words.** galaxies: elliptical and lenticular, cD – galaxies: evolution – galaxies: starburst – infrared: galaxies

## 1. Introduction

The ISOPHOT Serendipity Survey (ISOSS) (Bogun et al. 1996) has observed about 2000 galaxies at 170  $\mu\text{m}$ , providing a unique data base of far-infrared spectral energy distributions beyond 100  $\mu\text{m}$ . Stickel et al. (2000) found that *late type* galaxies generally contain a cold ( $T \sim 20$  K) dust component, with a wide range of infrared luminosities ( $10^9$ – $10^{12} L_{\odot}$ ). For *early type* galaxies, however, the traditional view is, that they are less dusty and less luminous in the infrared (see Knapp 1999 for a review).

We present a detailed study of the elliptical galaxy ISOSS J 15079+7247 detected by the ISOPHOT Serendipity Survey (ISOSS) as ultraluminous infrared source.

## 2. Observations

170  $\mu\text{m}$  photometry has been extracted from an ISOSS scan measurement performed with the C200 camera (Lemke et al. 1996), which provides a spatial resolution of  $1.5' FWHM$ . ISOSS J 15079+7247 is an unresolved point source with a flux density of  $F_{170\mu\text{m}} = 2.0$  Jy (Table 1), detected in a region of low galactic cirrus ( $I_{100\mu\text{m}} < 0.5$  MJy  $\text{sr}^{-1}$ , Schlegel et al. 1998). The source was centrally crossed by

the scan and detected by all four camera pixels. Within the positional errors of ISOSS ( $\sim 20''$  rms, Stickel et al. 2000), the source coincides in position with the IRAS point source F15080+7259, a 2MASS near-infrared source and a compact 1.2 mm continuum source detected by the MAMBO followup observations.

The 1.2 mm continuum measurements with MAMBO (Kreysa et al. 1998) at the IRAM 30 m telescope were carried out on October 23, 2001 under excellent conditions ( $\tau_{1.2\text{mm}} = 0.1$ ) in On–Off mode. Calibration measurements were obtained on the planets Mars and Uranus. The data were reduced with the NIC package including sky noise reduction, yielding a photometric accuracy of 20%.

CO(1–0) line observations were obtained with the IRAM 30 m telescope on March 3, 2002. The A100 and B100 heterodyne receivers were used simultaneously in position switching mode with system temperatures of 115 K. Both the  $512 \times 1$  MHz filterbank and the autocorrelator covered a range of  $1600 \text{ km s}^{-1}$  at the redshifted CO(1–0) line. The data were smoothed to resolutions of 10 MHz ( $32 \text{ km s}^{-1}$ ) for analysis, intensities are given in main beam brightness temperature,  $T_{\text{mb}}$ . For the 30 m telescope,  $T_{\text{mb}} = 1$  K corresponds to a flux density of 4.5 Jy from a point source in the 3 mm band.

Optical long slit spectra were obtained with the TWIN double spectrograph at the Calar Alto 3.5 m telescope on April 30, 2002 with spectral dispersions of 0.55  $\text{\AA}/\text{pixel}$  for the blue (3400–5500  $\text{\AA}$ ), 2.4  $\text{\AA}/\text{pixel}$  for the red (5500–9300  $\text{\AA}$ ) image channel and 1.5'' slit width. A relative spectrophotometric accuracy of 15% was obtained. The spectra were extracted according to the method of Horne (1986).

Send offprint requests to: O. Krause,  
e-mail: krause@mpia-hd.mpg.de

<sup>★</sup> Based on observations with the the IRAM 30 m Telescope, the Calar Alto Observatory and the Infrared Space Observatory ISO, an ESA project funded by Member States (especially France, Germany, The Netherlands and the UK) and with the participation of ISAS and NASA.

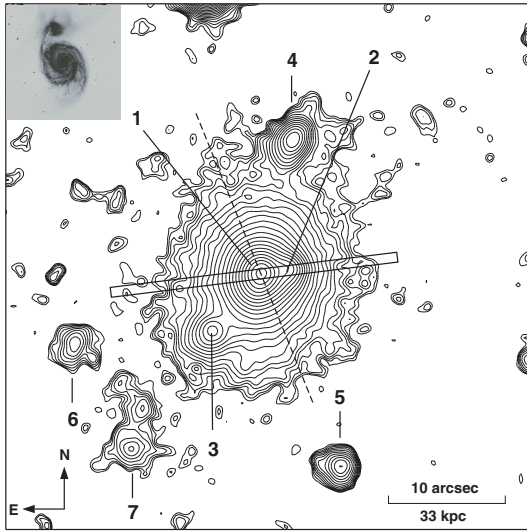


**Fig. 1.** *R*-band image of ISOSS J 15079+7247 obtained with the LAICA-camera at the Calar Alto 3.5 m telescope. The giant elliptical galaxy (1) shows two fainter brightness peaks (2) and (3) within the logarithmic contours. Several fainter objects in the surroundings are marked (4...7). The slit position of the spectroscopic observations (box) and the major axis of the elliptical (dashed line) are indicated. For comparison, an image of M51 scaled to the distance of ISOSS J 15079+7247 is shown in the upper left corner.

CCD images (pixel size  $0''.225$ ) were obtained with LAICA (Large Area Imager for Calar Alto) at the Calar Alto 3.5 m telescope in the *R*-band (seeing  $\sim 1.5''$ ). *I*-band photometry was performed with the MPIA 0.7 m telescope (pixel size  $0''.89$ ).

In addition, we included VLA 21 cm continuum data from Condon et al. (1998) and *JHK* near-infrared photometry from 2MASS (Cutri et al. 2000). 2MASS astrometry served as positional reference for the optical images and is accurate to  $0.5''$  rms.

### 3. Results

A deep optical *R*-band image (Fig. 1) shows an elliptical galaxy (1). The brightness profile can be well fitted by a de Vaucouleur  $r^{-1/4}$  law (Fig. 2) with an effective radius of  $r_e = 1.1 \pm 0.1''$ . The major/minor-axis ratio determined from a 2-dimensional de Vaucouleur fit is 1.2. The position of the brightness maximum (1) is (J2000) RA  $15^h07^m58.47^s \pm 0.1^s$ , Dec  $+72^\circ47'38.9'' \pm 0.5''$ . A second brightness peak (2) can be seen  $2.5''$  W, a third fainter one  $7''$  SE from the central peak. In addition, several fainter objects (4...7) are detected in the surroundings. The *R*-band brightness (Table 1) was integrated within a circular aperture of  $20''$  diameter and excluding source 4.

The elliptical galaxy coincides with an unresolved 1.2 mm continuum source. Strong emission was detected only in the central bolometer channel (beam size  $10''$ ), indicating a source size  $\leq 10''$  in the FIR/mm-continuum. No other source is seen in the MAMBO field (diameter  $\sim 100''$ ), which roughly covered the  $1.5'$  ISOPHOT beam. Within the positional errors, only the brightness peaks (1) and (2) of the *R*-band image are likely optical counterparts of the dust emission. The counterpart proposed

**Table 1.** Photometry of ISOSS J 15079+7247.

Band	Flux	Source
<i>R</i>	$17.44 \pm 0.15$ mag	LAICA, $20''$ aperture
<i>I</i>	$16.60 \pm 0.15$ mag	0.7m-Tel., $20''$ aperture
<i>J</i>	$15.7 \pm 0.2$ mag	determined from 2MASS images
<i>H</i>	$15.1 \pm 0.2$ mag	2MASS
<i>K</i>	$14.1 \pm 0.2$ mag	2MASS
$12 \mu\text{m}$	$< 54$ mJy	IRAS FSC
$25 \mu\text{m}$	$< 46$ mJy	IRAS FSC
$60 \mu\text{m}$	$0.53 \pm 0.08$ Jy	IRAS FSC
$100 \mu\text{m}$	$1.66 \pm 0.25$ Jy	IRAS FSC
$170 \mu\text{m}$	$2.0 \pm 0.6$ Jy	ISOPHOT $1.5'$ beam
$1200 \mu\text{m}$	$16.4 \pm 2.4$ mJy	MAMBO $11''$ beam
21 cm	5.3 mJy	Condon et al. (1998)

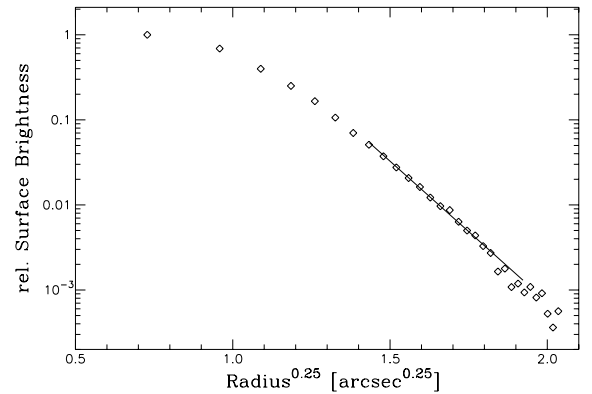


**Fig. 2.** *R*-band surface brightness as a function of (major axis) radius. A de Vaucouleurs law ( $r^{1/4}$ ) fits to the data, away from the very center determined by seeing or a central point source. The effective radius determined from the fit is  $3.5 \pm 0.2$  kpc.

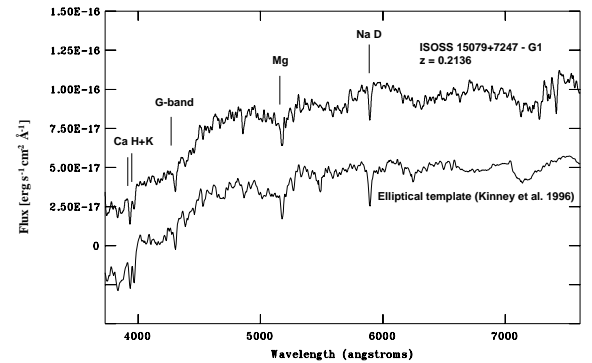


**Fig. 3.** Optical spectrum of ISOSS J 15079+7247 towards the bright nucleus of the elliptical galaxy (1). The used aperture (from  $3''$  E to  $1''$  W of the nucleus) avoids contamination by the emission region (2). The wavelength is given in the rest-frame ( $z = 0.2136$ ). The template spectrum of an evolved elliptical is shown for comparison.

by Moran et al. (1996), an M-star  $30''$  north of the elliptical, can now be also excluded.

In order to discriminate the two possible counterparts (1) and (2) kinematically, we have obtained long-slit spectra covering both brightness peaks. The data reveal a pure absorption spectrum (Fig. 3) towards the center of the elliptical (1). The redshift derived from Ca H & K, Na D and *G*-band feature is  $z = 0.2136 \pm 0.0005$ , corresponding to a luminosity distance  $D_L = 985$  Mpc (flat cosmology with  $\Omega_m = 0.3$ ,

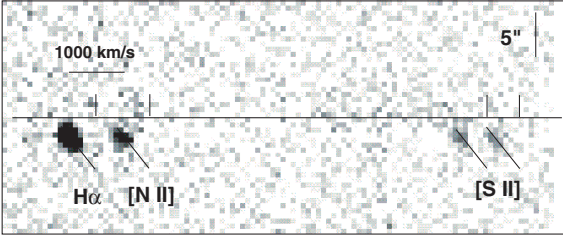


**Fig. 4.** Position-velocity image of gas emission from the companion (2). Spatial and velocity scales are indicated. The spectrum has been continuum subtracted for this image. The horizontal line marks the position of the elliptical nucleus. The vertical lines show the positions of  $H\alpha$ , [N II] and [S II] in the rest-frame of the elliptical. The tilted lines indicate the velocity gradient across the companion.

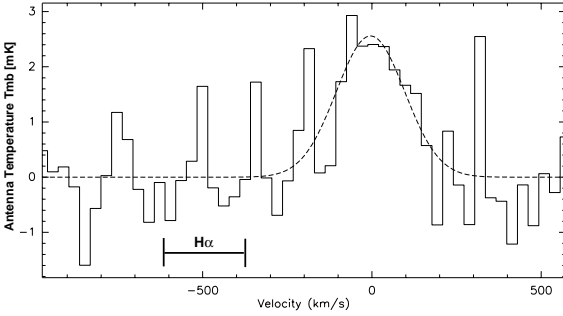


**Fig. 5.** CO (1–0) millimeter line spectroscopy of ISOSS J 15079+7247 obtained with the IRAM 30 m telescope. The zero point of velocity is set to the optical redshift of the elliptical galaxy. The range of the  $H\alpha$  emission line region of the companion (2) around  $-500 \text{ km s}^{-1}$  is indicated.

$\Omega_{\Lambda} = 0.7$  and  $H_0 = 75 \text{ km s}^{-1} \text{ Mpc}^{-1}$ ). In direction of the western brightness peak (2), an emission line spectrum is found (Fig. 4). The observed line strengths (Table 2) are consistent with a HII-type emission (Veilleux & Osterbrock 1987). The emission peak (2) is blue-shifted by  $478 \text{ km s}^{-1}$  with respect to the central elliptical. The spectral lines are oblique over a velocity range of  $\sim 250 \text{ km s}^{-1}$ , implying either rotation of a companion galaxy, mass outflow or infall towards the center of the elliptical.

The CO(1–0) spectrum (Fig. 5) obtained towards the continuum source shows a peak of emission at a redshift of  $0.2136 \pm 0.0001$ , coinciding with the optical redshift of the elliptical galaxy. The line width obtained from a Gaussian fit to the line is  $\Delta v = 250 \text{ km s}^{-1}$ . The integrated line area of  $0.61 \text{ K km s}^{-1}$  yields a molecular gas mass  $M(\text{H}_2) = 2.9 \times 10^{10} M_{\odot}$ . We used a conversion factor of  $4.6 M_{\odot} \text{ pc}^{-2} \text{ K}^{-1}$ , following Solomon et al. (1997). For some ULIRGs the conversion factor could be lower by a factor of 2–3 (Downes & Solomon 1998), which would lower the molecular gas masses by the same factor.

#### 4. Discussion

We now describe the overall characteristics of ISOSS J 15079+7247 and show that it is consistent with a gas-rich giant elliptical with a central starburst.

**Molecular gas:** The coincidence of observed CO line redshift with the optical redshift of the elliptical galaxy strongly suggest

**Table 2.** Observed emission lines in the optical spectrum of the star forming companion (2) of ISOSS J 15079+7247.

Line	Obs. Wavelength [Å]	Flux [ $10^{-16} \text{ erg cm}^{-2} \text{ s}^{-1} \text{ Å}^{-1}$ ]	
		observed	dereddened
[O II] 3726	4515.86	1.12	78.7
[O II] 3729	4519.16	0.57	40.1
H $\gamma$	5259.46	0.34	14.0
H $\beta$	5893.06	1.25	31.2
[O III] 5007	6068.60	0.98	21.7
[N II] 6548	7936.06	0.66	6.4
H $\alpha$	7953.79	9.49	90.9
[N II] 6584	7978.17	2.89	27.4
[S II] 6717	8139.98	1.29	11.6
[S II] 6731	8156.68	1.15	10.2

that the molecular gas is physically associated with this galaxy. Our  $R$ -band photometry closely represents the  $V$ -band brightness in the rest-frame of the elliptical. Applying a first order  $K$ -correction of  $K = 2.5 \log(1 + z)$  mag yields an absolute brightness of  $M_V \sim -22.7$  mag. This brightness and the effective radius  $r_e = 3.5 \text{ kpc}$  classify the galaxy as a giant elliptical. As shown in Figs. 3 and 6 the observed optical spectrum is well matched by the template spectrum of an evolved elliptical galaxy (Kinney et al. 1996; Bruzual & Charlot 1995). The very large molecular hydrogen mass of  $M(\text{H}_2) = 2.9 \times 10^{10} M_{\odot}$  is remarkable. So far, only significantly smaller amounts of molecular gas have been observed in ellipticals (e.g. Henkel & Wiklind 1997).

**High dust mass:** The far-infrared to millimeter spectral energy distribution (Fig. 6) can be fitted either by modified blackbody emission of *two optically thin* components with dust temperatures of 23 and 45 K (dashed line), or by *one single optically thick* modified blackbody of 42 K and optical depth  $\tau_{100 \mu\text{m}} = 3.5$  (solid line). We adopted a dust emissivity  $\beta = 2$  for the cold and  $\beta = 1.5$  for the warm dust component respectively. The derived dust masses for the optically thick and thin dust models are  $M_d = 5.4 \times 10^8 M_{\odot}$  and  $M_d = 2.5 \times 10^9 M_{\odot}$ , respectively. Since our 1.2 mm data correspond to a rest wavelength of  $990 \mu\text{m}$ , we used a dust mass absorption coefficient  $\kappa_{990 \mu\text{m}} = 0.64 \text{ cm}^2 \text{ g}^{-1}$  following Lisensfeld et al. (2000).

**Gas-to-dust mass ratio:** The derived high dust masses allow to determine the gas-to-dust mass ratios  $(M_{\text{H}_2} + M_{\text{HI}})/M_d$ , which are 20 and 110 for the optically thin and thick dust models, respectively (assuming  $M_{\text{H}_2} = M_{\text{HI}}$ ). If the gas-to-dust mass ratio is actually similar to the value of  $\sim 100$ – $300$  found for galaxies (Sodroski et al. 1997; Dunne & Eales 2001), this clearly favors the optically thick case. For a possibly lower CO-to- $\text{H}_2$  conversion factor this argument is strengthened.

**High star formation rate:** Assuming that a powerful starburst is the energy source of the infrared emission,  $L_{\text{FIR}}(40\text{--}1000 \mu\text{m}) = 1.9 \times 10^{12} L_{\odot}$  corresponds to a star formation rate of  $325 M_{\odot} \text{ yr}^{-1}$ , following Kennicutt (1998). The minimum radius of an optically thick blackbody sphere required to account for the integrated far-infrared luminosity is  $r_b = 600 \text{ pc}$ , following Klaas et al. (2001). As predicted by the FIR-radio correlation (Condon 1992), non-thermal emission from the starburst should be detected in the cm-continuum.

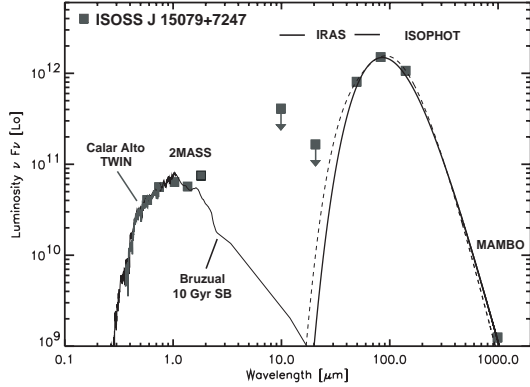


**Fig. 6.** Rest frame spectral energy distribution of ISOSS J 15079+7247, based on the fluxes and beams compiled in Table 1. The FIR dust emission can be well characterized by two dust models: One optically thick grey-body (solid) or the sum of two optically thin grey-bodies (dashed), see text for details. The optical and near-infrared emission can be fitted by a 10 Gyr old starburst following Bruzual & Charlot (1995).

Previous VLA observations by Condon et al. (1998) indeed show the presence of a compact continuum source at the position of the elliptical. The measured 21 cm flux density of 5.3 mJy yields a star formation rate of  $299 M_{\odot} \text{ yr}^{-1}$ , following Yun et al. (2001), and is consistent with the value derived from the far-infrared luminosity. No AGN is indicated, since ISOSS J 15079+7247 is both radio- and mid-infrared quiet.

**Opaque starburst:** The source was barely resolved at the VLA in the cm-continuum and the deconvolved size of  $\sim 1.5 \times 0.5 \text{ arcsec}^2$  ( $HWHM$ ) ( $= 4.8 \times 1.6 \text{ kpc}^2$ ) may be considered as upper limit for the starburst size, in agreement with our lower limit  $r_b = 0.6 \text{ kpc}$  from the far-infrared. Assuming an average radius of 1 kpc for the nuclear starburst and spherical distribution of dust and gas, we find a total column density of  $N(H) = 1.7 \times 10^{24} \text{ cm}^{-2}$  towards the center. This corresponds to a visual extinction of  $A_V \sim 1000 \text{ mag}$  and explains the absence of any optical emission lines towards the center of the elliptical, which is very unusual for ULIRGs (Veilleux et al. 1999).

**Role of companion galaxy:** The nearby brightness peak (2) included in the far-infrared measurements has a line spectrum and luminosity typical for a star-forming spiral. From the measured line ratios  $H\beta/H\alpha$  and  $H\gamma/H\beta$  (Table 2) we find an extinction of  $A_V = 3.0 \pm 0.2 \text{ mag}$ . We assumed recombination with an electron temperature of 10 000 K and low electron density  $\sim 10^2 \text{ cm}^{-3}$  as derived from our measured  $[SII] \lambda 6716/\lambda 6731$  and  $[OII] \lambda 3729/\lambda 3726$  ratios. In order to account for a flux loss due to the  $1.5''$  slit width, the measured fluxes have been scaled up by a factor of two (aperture correction at  $z \sim 0.2$  following Tresse & Maddox 1998). Then the star-formation rate derived from the dereddened  $H\alpha$  luminosity is  $14 M_{\odot} \text{ yr}^{-1}$  (following Kennicutt 1998). An independent estimate from  $[OII]$  emission yields  $18 M_{\odot} \text{ yr}^{-1}$ . The star formation rate in source (2) is by about an order of magnitude lower than the rate derived from the radio and far-infrared continuum of the whole source. In addition, the CO spectrum shows no line emission at the redshift of the companion galaxy as indicated in Fig. 5. We therefore conclude that the galaxy (2) is not the

source of the strong dust and gas emission. However, the object might be involved in an interaction or merger with the elliptical.

## 5. Conclusion

In the course of followup studies of the ISOPHOT Serendipity Survey we presented multi-wavelength observations showing that ISOSS J 15079+7247 is a gas- and dust rich elliptical galaxy with ultraluminous infrared emission. The amount of gas and dust is higher than in any other elliptical galaxy with comparable optical properties. Strikingly the starburst signatures of ISOSS J 15079+7247 are essentially hidden at optical wavelengths. This discovery shows that ellipticals can not be excluded as counterparts for luminous infrared galaxies.

**Acknowledgements.** The ISOPHOT Data Centre at MPIA is supported by Deutsches Zentrum für Luft- und Raumfahrt (DLR) with funds of Bundesministerium für Bildung und Forschung, grant No. 50QI0201. OK thanks the Wernher von Braun-Stiftung zur Förderung der Weltraumwissenschaften for financial support. We thank Michael Grewing and Clemens Thum for granting director's time at the IRAM 30 m telescope, Roland Gredel and Ulrich Thiele for director's time at Calar Alto, Josef Fried for providing LAICA data, Edward Moran for unpublished optical spectra and Hans Hippelein for valuable discussions. We are grateful to the anonymous referee for valuable comments. This research has made use of the NASA/IPAC Extragalactic Database (NED), which is operated by the Jet Propulsion Laboratory, California Institute of Technology, under contract with NASA.

## References

- Bogun, S., Lemke, D., Klaas, U., et al. 1996, *A&A*, 315, L71
- Bruzual, G. A., & Charlot, S. 1995, *Starburst Template Library in IRAF-STSDAS*
- Condon, J. J. 1992, *ARA&A*, 30, 575
- Condon, J. J., Yin, Q. F., Thuan, T. X., et al. 1998, *ApJ*, 116, 2682
- Cutri, R. M., Skrutskie, M. F., Van Dyk, S., et al. 2000, *Explanatory Supplement to the 2MASS Second Incremental Data Release*
- Downes, D., & Solomon, P. M. 1998, *ApJ*, 507, 615
- Dunne, L., & Eales, S. A. 2001, *MNRAS*, 327, 697
- Henkel, C., & Wiklind, T. 1997, *Space Sci. Rev.*, 81, 1
- Horne, K. 1986, *PASP*, 98, 609
- Klaas, U., Haas, M., Müller, S. A. H., et al. 2001, *A&A*, 379, 823
- Kennicutt, R. 1998, *ARA&A*, 36, 189
- Kinney, A. L., Calzetti, D., Bohlin, R. C., et al. 1996, *ApJ*, 467, 38
- Knapp, G. R. 1999, in *Star Formation in Early-Type Galaxies*, ed. P. Carral, & J. Cepa, *ASP Conf. Ser.*, 163, 119
- Kreysa, E., Gemuend, H.-P., Gromke, J., et al. 1998, *Proc. SPIE*, 3357, 319
- Lemke, D., Klaas, U., Abolins, J., et al. 1996, *A&A*, 315, L64
- Lisenfeld, U., Isaak, K. G., & Hills, R. 2000, *MNRAS*, 312, 433
- Moran, E., Halpern, J. P., & Helfand, D. J. 1996, *ApJSS*, 106, 341
- Schlegel, D. J., Finkbeiner, D. P., & Davis, M. 1998, *ApJ*, 500, 525
- Sodroski, T. J., Odegard, N., Arendt, R. G., et al. 1997, *ApJ*, 480, 173
- Solomon, P. M., Downes, D., Radford, S. J. E., et al. 1997, *ApJ*, 478, 144
- Stickel, M., Lemke, D., Klaas, U., et al. 2000, *A&A*, 359, 865
- Tresse, L., & Maddox, S. J. 1998, *ApJ*, 495, 691
- Veilleux, S., & Osterbrock, D. E. 1987, *ApJS*, 63, 295
- Veilleux, S., Kim, D.-C., & Sanders, D. B. 1999, *ApJ*, 522, 113
- Yun, S. M., Reddy, N. A., & Condon, J. J. 2001, *ApJ*, 554, 803